

Linking the quark meson model with QCD at high temperature

Jens Braun and Hans-Jürgen Pirner

Institut für Theoretische Physik, Universität Heidelberg, Philosophenweg 19, 69120 Heidelberg, Germany

Kai Schwenzer

Department of Physics, North Carolina State University, Raleigh, North Carolina 27695, USA

(Received 25 May 2004; published 22 October 2004)

We model the transition of a system of quarks and gluons at high energies to a system of quarks and mesons at low energies in a consistent renormalization group approach. Flow equations interpolate between the physics of the high-temperature degrees of freedom and the low-temperature dynamics at a scale of 1 GeV. We also discuss the dependence of the equation of state on baryon density and compare our results with recent lattice gauge simulations.

DOI: 10.1103/PhysRevD.70.085016

PACS numbers: 11.10.Wx, 11.30.Rd, 12.38.Mh

I INTRODUCTION

The equation of state of QCD in extreme conditions of high-temperature and/or high baryon density is at the focus of interest in heavy-ion collisions and astrophysics, i.e., neutron stars and supernovae. The current heavy-ion experiments at SPS (CERN) and RHIC (BNL) have challenged theoretical work on strong interactions at finite temperatures, due to the possible observation of new phases of matter. In particular, one expects a phase transition which separates a low-temperature region of hadrons from a high-temperature region of quarks and gluons, where both confinement is absent and chiral symmetry is restored. During the last years various direct numerical lattice simulations of QCD at finite-temperature and finite baryon density have been performed [1–3]. These computations are still limited to rather small lattices, therefore an alternative approach using an effective field theory is useful. The nonperturbative renormalization group (RG) flow equations present a practical alternative cf. [4]. Previously, we have discussed a linear σ -model with two massless quark flavors [5,6] which is treated with the renormalization group to capture the dynamics of the long-range fluctuations near the critical point correctly. In particular, this method includes dynamical chiral symmetry breaking as the dominating feature of QCD at low energies. The low-energy model lacks the gauge degrees of freedom, therefore it cannot be linked with lattice calculations for $T \geq 160$ MeV. As a first step, we propose to extend the flow equations of the linear σ -model by a flow equation for free massless quarks and gluons at high scale. By having an infrared cutoff for the QCD degrees of freedom we include confinement for the gluons in a poor man's way. Only gluons with high momenta are considered and consequently also the effective QCD coupling remains small in this domain. A perturbative calculation is then possible in principle [7].

Integrating these two systems with the same cutoff function successively over both high and low-energy excitations one obtains an adequate equation of state of strong interaction over a large range of temperatures and densities even without gluon interactions. We support this zero order calculation by comparing our results with recent lattice simulations. In addition, we argue that the lowest order corrections in the strong coupling constant make the transition between the two regimes less sensitive to the chosen scale where the two theories are sewn together. This method is similar to the approach in QCD sum rules where a perturbative high-energy sector is combined with a hadronic low-energy expansion. The independence on the matching scale is the key to a successful application of such a technique. Although the low-energy degrees of freedom do not arise dynamically as collective excitations of the fundamental gauge degrees of freedom, the smooth cutoff naturally interpolates between the different descriptions. In the last section we give a more detailed discussion of how the quark-meson system relates to the quark-gluon system, based on Ref. [8]. The benefit of our approach is to handle more complicated scenarios of strong interactions like the dependence of the equation of state on the quark mass or the finite volume of the system in a realistic way. The non-equilibrium thermodynamics of quarks and gluons may be another case [9] where semianalytic models help to elucidate the relevant time scales. Relativistic heavy-ion collisions cover both the quark-gluon plasma dynamics and the hadronic final stage, therefore a hybrid theory seems to be needed. The paper is organized as follows: In Sec. II we derive the flow equation for the chiral low-energy part. We propose a modified cutoff function, which allows us to perform the sum over the Matsubara frequencies analytically. In Sec. III we introduce the flow equation for the high-energy degrees of freedom and show that already the simple addition of the high and low-energy regime yields reasonable results for the ther-

modynamic quantities. A detailed discussion of the model and our conclusions are given in Sec. IV.

II. RG FLOW EQUATION FOR THE CHIRAL LOW-ENERGY PART

The $SU(2)_L \otimes SU(2)_R$ invariant linear σ -model with constituent quarks q and chiral mesons $\Phi = (\sigma, \vec{\pi})$ is an effective model for dynamical spontaneous chiral symmetry breaking at intermediate scales of $0 \leq k \leq \Lambda_M$. It is given by the Euclidean Lagrangian density

$$\mathcal{L}_{L\sigma M} = \bar{q}\not{\partial}q + g\bar{q}(\sigma + i\tau\pi\gamma_5)q + \frac{1}{2}(\partial_\mu\Phi)^2 + U(\Phi^2).$$

The grand canonical partition function Z for the quantum theory has the path integral representation

$$\begin{aligned} Z &= \text{Tr} e^{-\beta(H - \mu N)} \\ &= \int D\bar{q} \int Dq \int D\Phi \exp\left[-\int_0^\beta dt_E \right. \\ &\quad \left. \times \int d^3x_E (\mathcal{L}_{L\sigma M} - \mu q^\dagger q)\right], \end{aligned} \quad (1)$$

where periodic and antiperiodic boundary conditions apply for bosons and fermions, respectively. A Gaussian approximation to the path integral followed by a Legendre transformation yields the 1-loop effective action

$$\begin{aligned} \Gamma[\Phi, \bar{q}, q] &= S^{\text{uv}}[\Phi, \bar{q}, q] - \text{Tr} \log\left(\frac{\delta^2 S[\Phi, \bar{q}, q]}{\delta\bar{q}(x)\delta q(y)}\right) \\ &\quad + \frac{1}{2} \text{Tr} \log\left(\frac{\delta^2 S[\Phi, \bar{q}, q]}{\delta\Phi^i(x)\delta\Phi^j(y)}\right). \end{aligned} \quad (2)$$

Here, the boundary conditions of the functional integral appear in the momentum traces and we neglect contributions from mixed quark-meson loops. We consider the effective action Γ in a local potential approximation (LPA), which represents the lowest order in the derivative expansion and incorporates fermionic as well as bosonic contributions to the grand canonical potential density Ω . It is related to the pressure of the system by

$$\Omega(T, \mu) = -p(T, \mu). \quad (3)$$

To derive RG flow equations, we use Schwinger's proper-time method to regularize the respective logarithms. A straightforward partial evaluation of the trace in momentum space and a transformation of the expression to proper-time form yields

$$\begin{aligned} \Omega &= \Omega^{\text{uv}} + \frac{1}{2} \int \frac{d\tau}{\tau} T \sum_{n=-\infty}^{\infty} \int \frac{d^3p}{(2\pi)^3} \\ &\quad \times (4N_c N_f e^{-\tau[(\nu_n + i\mu)^2 + \vec{p}^2 + M_q^2]} - 3e^{-\tau(\omega_n^2 + \vec{p}^2 + M_\pi^2)} \\ &\quad - e^{-\tau(\omega_n^2 + \vec{p}^2 + M_\sigma^2)}) f(\tau k^2). \end{aligned} \quad (4)$$

where the Matsubara frequencies take the values $\omega_n = 2n\pi T$ for bosons and $\nu_n = (2n+1)\pi T$ for fermions, respectively. The effective masses are defined as

$$\begin{aligned} M_q^2 &= g^2\Phi^2, & M_\pi^2 &= 2\frac{\delta\Omega}{\delta\Phi^2}, \\ M_\sigma^2 &= 2\frac{\delta\Omega}{\delta\Phi^2} + 4\Phi^2\frac{\delta^2\Omega}{(\delta\Phi^2)^2}. \end{aligned}$$

A general set of smooth cutoff functions $f^a(\tau k^2)$, parametrized by a real positive number a , fulfills the required regularization conditions cf. Ref. [5,6,10]

$$f^{(a)}(\tau k^2) \equiv \frac{\Gamma(a+1, \tau k^2)}{\Gamma(a+1)}. \quad (5)$$

In previous works [5,6,10], cutoff functions with integer a have been applied to similar problems. However, in the case of a thermal system half-integer cutoff functions are better suited, since they effectively regularize only the spatial momentum integral. The relevant derivative of the cutoff function with respect to the IR-cutoff scale

$$k \frac{\partial f^{(a)}(\tau k^2)}{\partial k} = -\frac{2}{\Gamma(a+1)} (\tau k^2)^{a+1} e^{-\tau k^2}$$

involves a half-integer power of the proper-time variable τ , which combines with the half-integer power from the integration over the spatial momentum coordinates. Thus, we are able to perform the sum over the Matsubara frequencies *analytically*. We choose the smallest possible value for the cutoff parameter, $a = 3/2$. With $a = 3/2$ the RG improved flow equation for the grand canonical potential Ω reads

$$\begin{aligned} k \frac{\partial \Omega_{L\sigma M}(\Phi^2, k)}{\partial k} &= \frac{k^5}{6\pi^2} \left(\frac{3}{E_\pi} \left[\frac{1}{2} + n_B(E_\pi) \right] \right. \\ &\quad \left. + \frac{1}{E_\sigma} \left[\frac{1}{2} + n_B(E_\sigma) \right] \right. \\ &\quad \left. - \frac{2N_c N_f}{E_q} [1 - n_F(E_q) - \bar{n}_F(E_q)] \right). \end{aligned} \quad (6)$$

The appearing effective energies are defined by

$$E_i = \sqrt{k^2 + M_i^2}, \quad i \in \{\pi, \sigma, q\},$$

and the occupation numbers have the usual form

$$\begin{aligned} n_B(E) &= \frac{1}{e^{E/T} - 1}, & n_F(E) &= \frac{1}{e^{(E-\mu)/T} + 1}, \\ \bar{n}_F(E) &= \frac{1}{e^{(E+\mu)/T} + 1}. \end{aligned}$$

Note the exceptionally simple form of this evolution equation. One can immediately read off the contributions from the vacuum and thermal dynamics of the respective particles appearing with their proper degeneracy factors. Especially, compared to previous vacuum equations [10] energy denominators appear instead of the usual propa-

gator terms, which is natural for a thermal equation because of the broken Poincaré invariance. The analytic form of this equation allows a numerical solution, especially in the case of finite-temperature and density where the computational effort rises considerably.

Proper time flow equations are generally not exact but represent approximations to certain exact flows [11]. However, it has been shown that the corresponding vacuum equation with $a = 2$ [5,10] is equivalent to an optimized exact flow equation in LPA [12]. Because of its physically intuitive form, it is likely that an analogous correspondence holds between Eq. (6) and an appropriate exact RG flow.

The thermodynamics and phase structure of the chiral system has been discussed in [5,6,13]. One obtains a good description of the second-order chiral phase transition at $T_c \approx 160$ MeV and also a qualitative picture of the first-order phase transition at high densities. However, the model lacks the correct high-temperature behavior since it does not contain the appropriate degrees of freedom in this regime.

III. FLOW EQUATION FOR THE HIGH-ENERGY DEGREES OF FREEDOM

The fundamental degrees of freedom at high energies are quarks and gluons of QCD, described by the Euclidean Lagrangian density

$$\mathcal{L}_{\text{QCD}} = \bar{q}(\not{D} + m_c)q + \frac{1}{4}F_{\mu\nu}F_{\mu\nu} + \mathcal{L}_{gf} + \mathcal{L}_{\text{ghost}}, \quad (7)$$

where m_c is the respective quark mass matrix and \mathcal{L}_{gf} and $\mathcal{L}_{\text{ghost}}$ denote the gauge-fixing-term and the ghost-term, respectively. Because of asymptotic freedom, quarks and gluons decouple at asymptotically high energies. Lattice gauge simulations cf. Ref. [1,2] suggest that even at moderate temperatures, $T \gtrsim 200$ MeV, the equation of state of the interacting system behaves almost like a free gas. Therefore in a first attempt to link the quark-meson model with QCD we neglect the full gauge interactions and approximate the high-energy part of QCD at scales $k > \Lambda_M$ by a free gas of massless quarks and gluons. In the following we work in the Feynman-gauge and neglect a possible running of the gauge parameter.

The integration of the thermal quark and gluon fluctuations within the RG flow using the same smooth infrared cutoff function, $a = 3/2$, allows a smooth transition of the respective degrees of freedom. Cutoff functions with higher values for “ a ” give a slightly higher gluon pressure near the critical temperature. The infrared cutoff has the same effect as a self-interaction of the gluons and provides an effective screening for the gluonic degrees of freedom. In this section we show that already the simple addition of the free quark-gluon flow to the meson flow gives reasonable results for certain quantities as the equation of state. We will discuss the matching of the quark-

meson model with the quark-gluon model in the last section.

We neglect the current quark masses for the two light quark flavors. Then the equation for the high-energy part has a very compact form in our simplified approximation

$$\begin{aligned} k \frac{\partial \Omega_{\text{QCD}}(k)}{\partial k} &= \frac{k^4}{6\pi^2} \left(N_g \left[\frac{1}{2} + n_B(k) \right] - 2N_c N_f \right. \\ &\quad \left. \times [1 - n_F(k) - \bar{n}_F(k)] \right) \\ &= k^4 \sum_{i \in \{g, q, \bar{q}\}} \frac{N_i}{6\pi^2} \left[\frac{s_i}{2} + n_i(k) \right]. \end{aligned} \quad (8)$$

The sum runs over gluons, quarks and antiquarks including the appropriate occupation numbers with degeneracy factors and sign factors $N_g = 16$, $s_g = +1$ for the bosons and $N_q = N_{\bar{q}} = 2N_c N_f = 12$, $s_q = s_{\bar{q}} = -1$, for the fermions and antifermions, respectively. The potential of the total system is obtained by integrating the quark-gluon evolution equation from $k = \Lambda_\infty$ to $k = \Lambda_M$ and the quark-meson evolution equation from $k = \Lambda_M$ to $k = 0$, i.e., the IR-cutoff parameter of the quark-gluon potential is identical to the UV-cutoff parameter of the quark-meson model. We can integrate the simplified QCD flow equation analytically and get

$$\begin{aligned} \Omega_{\text{QCD}}(\Lambda_\infty, \Lambda_M, T) &= \sum_i s_i \frac{N_i}{6\pi^2} \left\{ \frac{k^4}{8} - k^3 T Li_1[s_i n_i^\infty(k)] \right. \\ &\quad - 3k^2 T^2 Li_2[s_i n_i^\infty(k)] \\ &\quad - 6kT^3 Li_3[s_i n_i^\infty(k)] \\ &\quad \left. - 6T^4 Li_4[s_i n_i^\infty(k)] \right\}_{\Lambda_\infty}^{\Lambda_M}. \end{aligned} \quad (9)$$

The polylogarithmic functions $Li_n(x)$ are defined by

$$Li_1(x) = -\ln(1-x), \quad Li_n(x) = \int_0^x \frac{Li_{n-1}(z)}{z} dz$$

and the functions $n_i^\infty(k)$ denote the classical Maxwell-Boltzmann distribution functions of the respective particles

$$\begin{aligned} n_g^\infty(k) &= e^{-k/T}, & n_q^\infty(k) &= e^{-(k-\mu)/T}, \\ n_{\bar{q}}^\infty(k) &= e^{-(k+\mu)/T}. \end{aligned}$$

We can evaluate Eq. (9) in the limit $\Lambda_\infty \rightarrow \infty$ by making use of the behavior of the polylogarithms in the vicinity of zero:

$$\Omega_{\text{QCD}}(\Lambda_\infty, \Lambda_M, T) = \sum_i s_i \frac{N_i}{6\pi^2} \left(-\frac{\Lambda_\infty^4}{8} + \frac{\Lambda_M^4}{8} - \Lambda_M^3 T Li_1[s_i n_i^\infty(\Lambda_M)] - 3\Lambda_M^2 T^2 Li_2[s_i n_i^\infty(\Lambda_M)] - 6\Lambda_M T^3 Li_3[s_i n_i^\infty(\Lambda_M)] - 6T^4 Li_4[s_i n_i^\infty(\Lambda_M)] \right). \quad (10)$$

Here we kept the divergent part proportional to Λ_∞^4 , so the potential still needs to be regularized. In the limit of zero temperature the vacuum part can be identified, since it is only a function of Λ_M and Λ_∞ :

$$\Omega_{\text{QCD}}^{\text{vac}}(\Lambda_\infty, \Lambda_M, T = 0) = \sum_i s_i \frac{N_i}{6\pi^2} \left(\frac{\Lambda_M^4}{8} - \frac{\Lambda_\infty^4}{8} \right). \quad (11)$$

To obtain the potential $\Omega_{L\sigma M}$ of the chiral low-energy part, we integrate the corresponding flow equation from $k = \Lambda_M$ to $k = 0$. We switch the degrees of freedom at a scale $\Lambda_M = 1.0$ GeV where the gauge degrees of freedom become unreliable and below which the physics can be described by the chiral model. As initial values for the low-energy part at this scale we choose $U(\Phi^2) = \frac{1}{2}m_M^2\Phi^2 + \frac{1}{4}\lambda_M\Phi^4$ with $\lambda_M = 37$, $m_M = 320$ MeV and the quark-meson coupling $g = 3.45$. These initial parameters are adjusted to get the value of the pion decay constant $\langle\sigma\rangle = f_\pi = 88$ MeV at $k = 0$ in the chiral limit and a quark mass of roughly 300 MeV. In principle, the starting parameters should result from the integration over the QCD degrees of freedom. This may be possible including quark interactions from gluons at higher scales.

The full potential reads

$$\Omega_{\text{total}}(\Lambda_\infty, k = 0, T) = \Omega_{\text{QCD}}(\Lambda_\infty, \Lambda_M, T) + \Omega_{L\sigma M}(\Lambda_M, k = 0, T). \quad (12)$$

The finite-temperature part relevant for the pressure does not depend on the vacuum energy. Therefore in the regularized potential the UV-divergent part drops out as it must and

$$p(T) = -\Omega_{\text{total}}(\Lambda_\infty, k = 0, T) + \Omega_{\text{total}}(\Lambda_\infty, k = 0, T = 0). \quad (13)$$

In the limit of infinite temperature $T \rightarrow \infty$ the ratio of p/T^4 yields the Stefan-Boltzmann limit for a massless quark-gluon gas, because the region $k < \Lambda_M$ has vanishing weight

$$\frac{p(T)}{T^4} \rightarrow \left[N_g + \frac{7}{8}(N_q + N_{\bar{q}}) \right] \frac{\pi^2}{90}. \quad (14)$$

For small temperatures $T \rightarrow 0$ we find a massless gas of pions with

$$\frac{p(T)}{T^4} \rightarrow 3 \frac{\pi^2}{90}. \quad (15)$$

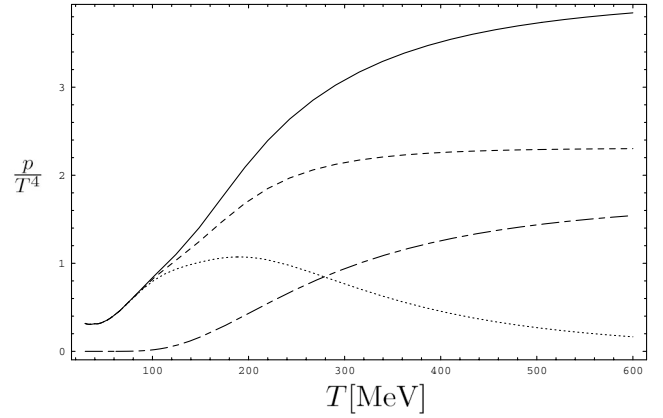


FIG. 1. Different contributions to p/T^4 arising from the mesons and quarks (constituent quarks and free quarks) (dashed line) and the gluons (dash-dotted line). The dotted line shows the scaled pressure function of the linear σ -model with two quark flavors which contains the cutoff Λ_M .

In Fig. 1 we show the different contributions to p/T^4 arising from the integration over the flow of the mesons and all quark contributions (including both the constituent quarks with cutoff Λ_M and free quarks without cutoff) (dashed line) and the integration over the gluons (dash-dotted line). Furthermore we plot the scaled pressure of the linear σ -model with cutoff Λ_M (dotted line) described by Eq. (6).

The comparison indicates clearly that the quark-meson model with cutoff Λ_M alone becomes unreliable for a description of the equation of state at temperatures $T > 150$ MeV. It definitely has to be linked with quark and gluon degrees of freedom at higher temperatures. The linear sigma model is adequate at low-temperature where massless pions dominate the pressure and the quarks are massive due to spontaneous breaking of the chiral symmetry. Gluons contribute to the pressure only at rather high temperatures since the smooth infrared cutoff around the scale Λ_M introduces a gluon mass and gives deviations between our model and the free gluon gas.

IV. DETAILED RESULTS AND DISCUSSION OF THE MODEL

The flow equation with the successive integration over different degrees of freedom avoids a first-order transition which typically arises in simplified models with two components like the bag model combined with a pion gas [14].

The critical behavior of the system is described by the pion decay constant which is shown as a function of temperature for vanishing chemical potential in Fig. 2. The figure shows that the pion decay constant goes to zero for $T_c = 154$ MeV continuously. For temperatures below T_c the quarks are massive and the pions are massless, so the system is in the chiral broken phase. For temperatures

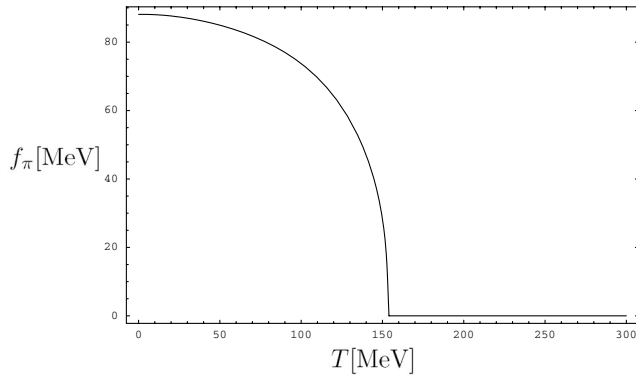


FIG. 2. The pion decay constant as a function of temperature for vanishing chemical potential. The dynamics of the phase transition arise entirely from the quark-meson sector in our model, since the quark-gluon interaction is neglected in the QCD sector.

above T_c the system is in the chiral symmetric phase, where the quarks are massless and the pions are massive. Thereby one obtains a second-order chiral phase transition at $T = T_c$, which is about 20 MeV smaller than the result of lattice calculations [2]. Note that the pion decay constant as a function of temperature for the chiral low-energy system does not differ from the function of the total system, because the pion decay constant is zero in the high-energy part of our model. In Fig. 3 we compare the curve of the scaled energy ϵ/T^4 with 3 times the pressure $3p/T^4$ as a function of temperature. Both quantities ϵ/T^4 and $3p/T^4$ gradually increase across the second-order phase transition. The scaled pressure density reaches about 95% of the Stefan-Boltzmann limit at $T \approx 4T_c$, whereas respective lattice calculations [2] reach about 85%. The energy density becomes more rapidly

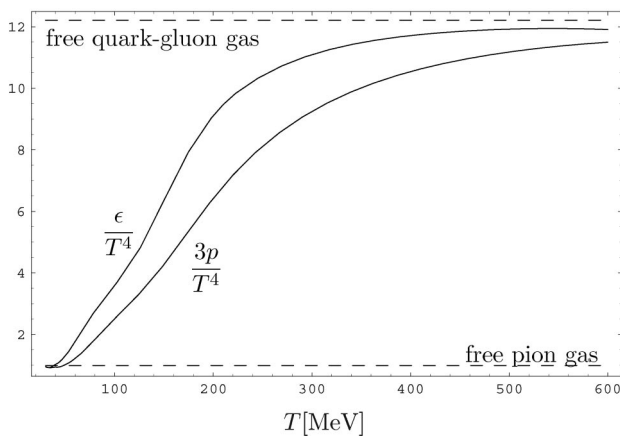


FIG. 3. The scaled pressure multiplied by a factor of 3 compared to the scaled energy density as a function of temperature. The upper and lower Stefan-Boltzmann limits corresponding to a free quark-gluon gas and a pion gas are drawn as dashed lines.

asymptotic cf. Figure 3. Thereby, the “interaction measure” $\epsilon - 3p$ has a peak at $T \approx 1.27T_c \approx 196$ MeV, whereas the respective maximum of lattice calculations of (2 + 1)-flavor QCD [3] is located at approximately $T \approx 1.1T_c \approx 189$ MeV. The interaction measure $\epsilon - 3p$ has more subtle features at finite chemical potential. For instance, we find a low-temperature maximum in $\epsilon - 3p$ at finite chemical potential which does not agree with finite density lattice calculations. This low-temperature maximum arises from the fact that we have constituent quarks in our model and no baryons for temperatures below T_c . Lattice calculations of the same quantity go rapidly to zero for temperatures below T_c which may be an effect of confinement and/or of the limited grid sizes and the high masses of the nucleons.

To study the effects of a finite baryon chemical potential on the pressure it is useful to consider the difference Δp of the pressure of the system at finite and vanishing chemical potential and the same temperature, respectively:

$$\Delta p = [p(T, \mu) - p(T, \mu = 0)]. \quad (16)$$

Small chemical potentials compared to the baryon mass suppress the baryonic pressure at low temperatures. Our calculation shows a suppression of $\Delta p/T^4$ in agreement with the low-temperature expansion for a gas of non-relativistic and noninteracting constituent quarks with masses $m > \mu = \mu_B/3$, which reads

$$\frac{\Delta p}{T^4} = \frac{g}{2\sqrt{2}\pi^{3/2}} \left(\frac{m}{T}\right)^{3/2} (e^{-(m-\mu)/T} - e^{-m/T}). \quad (17)$$

Here g denotes the degeneracy factor of the fermions. In Fig. 4 one can see the scaled pressure $\Delta p/T^4$ of the quarks for different chemical potentials $\mu_B = 100$ MeV to $\mu_B = 530$ MeV. We have chosen these values identical to the ones in the lattice calculation in Ref. [3], where the equation of state includes heavy strange quarks. At high

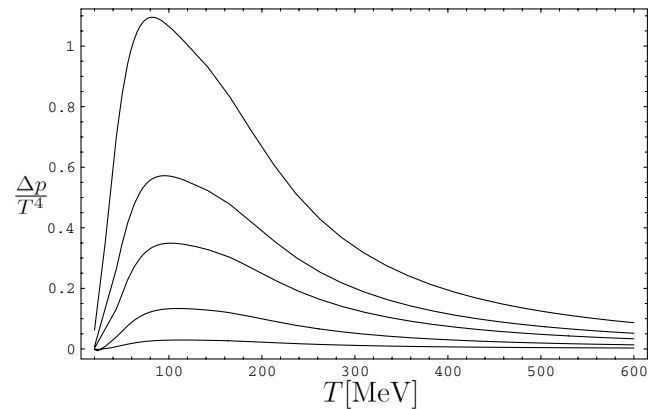


FIG. 4. The scaled pressure difference $\Delta p/T^4 = [p(T, \mu) - p(T, \mu = 0)]/T^4$ is shown as a function of temperature for $\mu_B = 100, 210, 330, 410, 530$ MeV (from bottom to top).

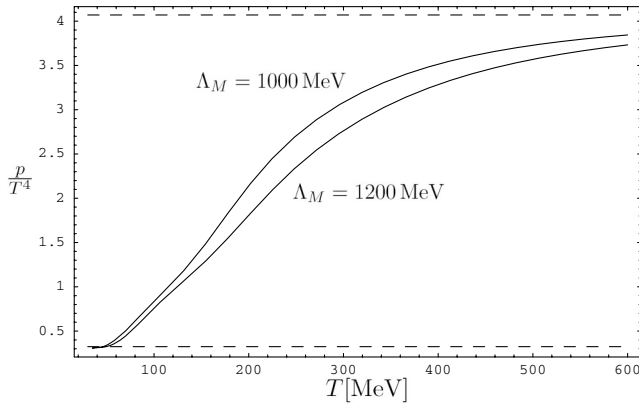


FIG. 5. The scaled pressure as a function of temperature for two different sets of initial parameters. The upper curve shows the scaled pressure for $\Lambda_M = 1000$ MeV. The lower curve represents the result for the scaled pressure, if one changes the transition scale from $\Lambda_M = 1000$ MeV to $\Lambda_M = 1200$ MeV but keeps all other parameters fixed. The upper and lower dashed line shows the Stefan-Boltzmann limit for a free quark-gluon gas and a free pion gas, respectively.

temperatures the scaled pressure difference decreases according to

$$\frac{\Delta p}{T^4} = 4N_c N_f \left(\frac{\mu^2}{24T^2} + \frac{\mu^4}{48\pi^2 T^4} \right). \quad (18)$$

This behavior is also reproduced by our calculation cf. Figure 4.

Let us finally discuss the matching between the quark-gluon and quark-meson sector by including QCD dynamics on the high-energy side [8,15–18]. In Fig. 5 we show the scaled pressure as a function of the temperature for two different matching scales $\Lambda_M = 1000$ MeV and $\Lambda_M = 1200$ MeV when we sew the two flow equations together as described in the paper. No readjustment is made. The scaled pressure increases when the infrared cutoff is lowered. For the gluon system the fade out of the colored degrees of freedom sets in at lower momenta whereby gluons contribute more pressure. A lower cutoff also postpones the breaking of chiral symmetry and therefore the quarks become less massive and contribute more to the pressure at low temperatures.

In the quark-gluon regime the first-order correction from gluon radiation to the scaled pressure is well known [19]:

$$\Delta \frac{p}{T^4} = -g^2 \left(\frac{1}{9} + \frac{5}{72} \right). \quad (19)$$

Here the sum includes the gluon and quark degrees of freedom and g^2 runs approximately as $g^2(\Lambda_M^2 + T^2)$ [7]. Therefore the gluon correction is larger negative for the lower cutoff bringing the two curves with the scaled pressure closer to each other. In the meson regime the

main effect of a lower cutoff is the change of the effective four fermion coupling which corresponds in the bosonized theory to a change of the boson mass. In Ref. [8] the evolution of the four fermion coupling has been derived. Neglecting subleading terms, the respective evolution equation for the inverse scaled four fermion interaction $\tilde{\epsilon}$ reduces to

$$k \frac{\partial \tilde{\epsilon}}{\partial k} = \frac{3}{8\pi^2} - \left(2 - \frac{4g^2}{4\pi^2} \right) \tilde{\epsilon} + \frac{40}{3} \frac{g^4}{16\pi^2} \tilde{\epsilon}^2, \quad (20)$$

with

$$\tilde{\epsilon} = \frac{2m^2}{g^2 k^2}. \quad (21)$$

The right-hand side of the evolution equation has two zeros at $\tilde{\epsilon} = \tilde{\epsilon}_1$ and $\tilde{\epsilon} = \tilde{\epsilon}_2$ with $\tilde{\epsilon}_1 < \tilde{\epsilon}_2$. The starting value $\tilde{\epsilon}(\Lambda_M)$ lies to the left of $\tilde{\epsilon}_1$ and the flow equation causes $\tilde{\epsilon}$ to decrease, i.e., $\tilde{\epsilon}(\Lambda_M - dk) < \tilde{\epsilon}(\Lambda_M)$. This change produces a growing four fermion interaction which will evolve the system faster to the chiral symmetry breaking point with k . Consequently the evolution below the symmetry breaking scale and with it the low-temperature scaled pressure will be approximately reproduced when we readjust the four fermion coupling in agreement with the evolution equation $d\tilde{\epsilon}/dk$. Although, high-temperature and low-temperature physics depend on the matching scale, gluon radiative corrections reduce the dependence on the scale Λ_M in both regimes.

Nevertheless, one must be cautious. We cannot fully abolish the matching scale, because then we would run the QCD coupling too deep into the infrared where it becomes undefined. Moreover, the above results come from a different cutoff scheme than the heat kernel cutoff. Since there exists not yet a fully consistent treatment of gluon radiative corrections using a heat kernel cutoff, this needs further work.

Linking the quark-meson model with QCD degrees of freedom we find that the low-energy sigma model can be extended to high-temperature $T > 150$ MeV. The combination of different degrees of freedom within a single renormalization group flow opens the window for a consistent description of QCD both at low and high scales which is needed in the equation of state. Already the simplified model we constructed shows good agreement with lattice simulations. As indicated above, the matching of the low-energy model with the quark-gluon sector can be improved to get an equation of state that is largely independent of the precise value of the matching scale.

ACKNOWLEDGMENTS

The authors would like to thank H. Gies and C. Wetterich for discussions about the matching between QCD and the linear sigma model.

- [1] G. Boyd, J. Engels, F. Karsch, E. Laermann, C. Legeland, M. Lutgemeier, and B. Petersson, Nucl. Phys. **B469**, 419 (1996).
- [2] F. Karsch, E. Laermann, and A. Peikert, Phys. Lett. B **478**, 447 (2000).
- [3] Z. Fodor, Nucl. Phys. **A715**, 319 (2003).
- [4] J. Berges, N. Tetradis, and C. Wetterich, Phys. Rep. **363**, 223 (2002).
- [5] B.J. Schaefer and H.J. Pirner, Nucl. Phys. **A660**, 439 (1999).
- [6] J. Meyer, G. Papp, H.J. Pirner, and T. Kunihiro, Phys. Rev. C **61**, 035202 (2000).
- [7] D.H. Rischke, J. Schaffner, M.I. Gorenstein, A. Schaefer, H. Stoecker, and W. Greiner, Z. Phys. C **56**, 325 (1992).
- [8] H. Gies and C. Wetterich, Phys. Rev. D **69**, 025001 (2004).
- [9] J. Berges, S. Borsanyi, and J. Serreau, Nucl. Phys. **B660**, 51 (2003).
- [10] J. Meyer, K. Schwenzer, H.J. Pirner, and A. Deandrea, Phys. Lett. B **526**, 79 (2002).
- [11] D. F. Litim and J. M. Pawłowski, Phys. Rev. D **66**, 025030 (2002).
- [12] D. F. Litim, Phys. Rev. D **64**, 105007 (2001).
- [13] K. Schwenzer and H.J. Pirner, contribution to *Proceedings of the Workshop on Strong and Electroweak Matter (SEWM 2002), Heidelberg, Germany*, edited by Michael G. Schmidt (World Scientific, Singapore, 2003).
- [14] A. Chodos, R. L. Jaffe, K. Johnson, C. B. Thorn, and V. F. Weisskopf, Phys. Rev. D **9**, 3471 (1974).
- [15] H. Gies and C. Wetterich, Phys. Rev. D **65**, 065001 (2002).
- [16] E. Meggiolaro and C. Wetterich, Nucl. Phys. **B606**, 337 (2001).
- [17] H.J. Pirner, Prog. Part. Nucl. Phys. **29**, 33 (1992).
- [18] H. Arodz and H.J. Pirner, Acta Phys. Pol. B **30**, 3895 (1999).
- [19] J.I. Kapusta, *Finite-Temperature Field Theory* (Cambridge University Press, England, 1989).